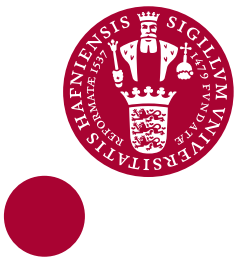

Phase contrast mapping MRI measurements of global cerebral blood flow across different perfusion states – A direct comparison with 15O-H2O positron emission tomography using a hybrid PET/MR system

Puig, Oriol; Vestergaard, Mark B; Lindberg, Ulrich; Hansen, Adam E; Ulrich, Annette; Andersen, Flemming L; Johannesen, Helle H; Rostrup, Egill; Law, Ian; Larsson, Henrik B.; Henriksen, Otto M

Published in:
Journal of Cerebral Blood Flow and Metabolism

DOI:
10.1177/0271678X18798762

Publication date:
2019

Document version
Publisher's PDF, also known as Version of record

Original Article

JCBFM

Journal of Cerebral Blood Flow & Metabolism
0(00) 1–11

DOI: 10.1177/0271678X18798762
journals.sagepub.com/home/jcbfm
SAGE

Phase contrast mapping MRI measurements of global cerebral blood flow across different perfusion states – A direct comparison with ^{15}O-H_2O positron emission tomography using a hybrid PET/MR system

Oriol Puig[1], Mark B Vestergaard[1], Ulrich Lindberg[1], Adam E Hansen[1], Annette Ulrich[2], Flemming L Andersen[1], Helle H Johannesen[1], Egill Rostrup[1], Ian Law[1], Henrik BW Larsson[1] and Otto M Henriksen[1]

Abstract

Phase-contrast mapping (PCM) magnetic resonance imaging (MRI) provides easy-access non-invasive quantification of global cerebral blood flow (gCBF) but its accuracy in altered perfusion states is not established. We aimed to compare paired PCM MRI and ^{15}O-H_2O positron emission tomography (PET) measurements of gCBF in different perfusion states in a single scanning session. Duplicate combined gCBF PCM-MRI and ^{15}O-H_2O PET measurements were performed in the resting condition, during hyperventilation and after acetazolamide administration (post-ACZ) using a 3T hybrid PET/MR system. A total of 62 paired gCBF measurements were acquired in 14 healthy young male volunteers. Average gCBF in resting state measured by PCM-MRI and ^{15}O-H_2O PET were 58.5 ± 10.7 and 38.6 ± 5.7 mL/100 g/min, respectively, during hyperventilation 33 ± 8.6 and 24.7 ± 5.8 mL/100 g/min, respectively, and post-ACZ 89.6 ± 27.1 and 57.3 ± 9.6 mL/100 g/min, respectively. On average, gCBF measured by PCM-MRI was 49% higher compared to ^{15}O-H_2O PET. A strong correlation between the two methods across all states was observed ($R^2 = 0.72$, $p < 0.001$). Bland–Altman analysis suggested a perfusion dependent relative bias resulting in higher relative difference at higher CBF values. In conclusion, measurements of gCBF by PCM-MRI in healthy volunteers show a strong correlation with ^{15}O-H_2O PET, but are associated with a large and non-linear perfusion-dependent difference.

Keyword

^{15}O-H_2O, cerebral blood flow, phase contrast mapping, positron emission tomography, magnetic resonance imaging

Received 16 February 2018; Revised 25 May 2018; Accepted 29 July 2018

Introduction

Quantitation of cerebral blood flow (CBF) is essential in the study of brain pathologies and, even more, of brain physiology. The generally accepted reference method for CBF quantification in humans is ^{15}O-H_2O positron emission tomography (PET),[1] but it is technically challenging to perform as it requires both online production of the radiotracer and arterial cannulation. The use of ^{15}O-H_2O PET is therefore limited to highly specialized centers and selected clinical and research applications.

[1]Department of Clinical Physiology, Nuclear Medicine and PET, Copenhagen University Hospital Rigshospitalet, Copenhagen, Denmark
[2]Department of Cardiothoracic Anesthesiology, Copenhagen University Hospital Rigshospitalet Blegdamsvej, Copenhagen, Denmark

Corresponding author:
Oriol Puig, Department of Clinical Physiology, Nuclear Medicine and PET, Rigshospitalet Blegdamsvej 9, Copenhagen 2100, Denmark.
Email: oriol.puig.calvo@regionh.dk

Phase contrast mapping (PCM) magnetic resonance imaging (MRI) allows fast, non-invasive, and reproducible measurements of blood flow in the arteries feeding the brain.[2] By normalizing the PCM measurements of total blood flow (in mL/min) to brain weight, global CBF (gCBF) can be calculated (in mL/100 g/min). Due to its simplicity, PCM MRI measurements of gCBF are increasingly being applied both in large population studies[3,4] and in quantitative studies of cerebrovascular physiology.[5] By combing PCM MRI with susceptibility-based MRI oximetry, or similar MRI techniques for the quantification of blood oxygenation, global cerebral oxygen consumption can be quantified.[6] Using such combined MRI approaches, a number of articles have investigated the influence of aging[7] and of various acute interventions on cerebral oxygen metabolism.[8,9] PCM MRI may also be used for the scaling of relative MRI CBF measurements obtained by the dynamic susceptibility contrast MRI[10] or arterial spin labelling (ASL) MRI.[11,12]

However, despite its popularity and widespread use, validation studies of gCBF measurements by PCM MRI with accepted reference methods are sparse. In previous studies, PCM MRI measurements of gCBF have proven to be in fair agreement with gCBF values from the literature.[3,13] An early study comparing gCBF measurements obtained by ^{15}O-H_2O PET and PCM MRI failed to find a significant correlation between values obtained by the two techniques, but it should be noted that the measurements were performed months apart.[14] A more recent study comparing same-day PCM MRI and ^{15}O-H_2O PET measurements, showed a strong positive correlation between gCBF measurements in *resting* state, but demonstrated also that PCM MRI yielded 63% higher gCBF values measurements compared to ^{15}O-H_2O PET.[15] However, the behavior of PCM measurements against an accepted reference method in a broader range of CBF values, e.g. during induced hypo- and hyperperfusion, has not been established. Such knowledge is essential when interpreting PCM MRI-dependent studies of cerebral perfusion or oxygen metabolism during various interventions.

A recent review highlighted the importance of the time interval between CBF measurements in method comparison studies by showing that the method agreement increases when the measurements are performed in close sequence.[16] With the introduction of hybrid PET/MRI scanners, simultaneous PET and MRI CBF measurements can now be performed under identical physiological conditions eliminating important sources of variability between the measurements in acutely altered perfusion states, which may be difficult to replicate when performing sequential imaging on separate systems.

The aim of this study was to compare PCM MRI against fully quantitative ^{15}O-H_2O PET measurements of gCBF in resting state and in altered perfusion states with a hybrid PET/MRI scanner. Furthermore, we utilized the short 2 min half-life to obtain multiple paired observations by repetitive tracer injections as has been done in piglets.[17]

Material and methods

Fourteen healthy young males (mean age 23.9 ± 2 years, range 21 – 28 years) were enrolled in the study. Inclusion criteria were: healthy males between 18 and 35 years old. Exclusion criteria were: contraindications to MRI or arterial cannulation, a medical history of prior or current neurological or psychiatric disease, or severe head trauma. The rationale for studying only males was to study a population as homogeneous as possible and to benefit from the slightly larger vessel diameter in males.

The study was approved by the Danish National Committee of Health Research Ethics (H-16023156) and was conducted according to the Declaration of Helsinki II. Written informed consent was obtained from all the participants.

Experiment setup

All PET and MR imaging were obtained on a 3T Siemens Biograph mMR hybrid PET/MR system (Siemens Healthcare, Erlangen, Germany) within a single scanning session lasting approximately 2.5 h. Volunteers were instructed not to consume coffee, tea, chocolate or any other caffeine containing beverages 8 h prior to the experiment because of the CBF modulating effects.[18] Before the scan, a light meal was offered to all the participants.

Immediately before or after the PET/MRI scan, a low radiation CT scan (120 kV, 30 mAs, 5-mm slice width) was performed in a PET/CT scanner (Siemens Biograph, Siemens, Erlangen, Germany) and was used for the attenuation correction of the PET images.[19]

An arterial catheter was placed in the radial artery of the non-dominant hand to allow for arterial blood sampling, and a venous line was placed in the median cubital vein of the dominant forearm for the administration of radiotracer and acetazolamide (ACZ). Foam padding was placed around the head to minimize head motion during the experiment and earplugs were used to reduce the ambient noise.

Duplicate combined CBF PET/MRI measurements were performed in resting condition, hypoperfusion and hyperperfusion as shown in Figure 1. To induce hypoperfusion, volunteers were instructed to breathe deeply at a respiratory rate of 24 respirations per minute.

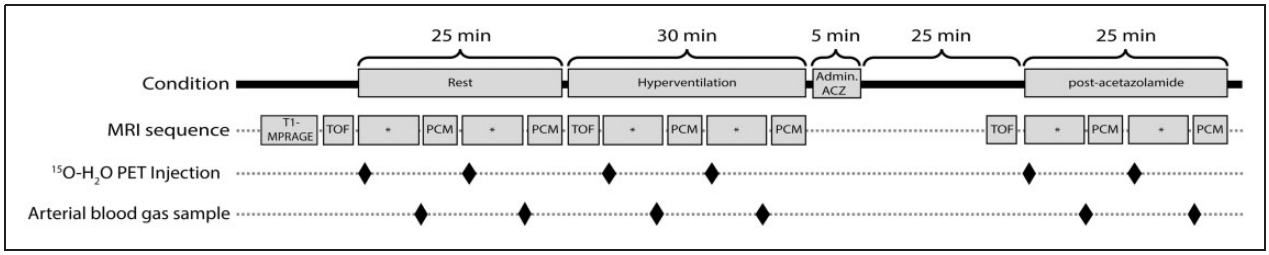

Figure 1. Experiment overview.
PCM: phase contrast mapping; ACZ: acetazolamide; TOF: time of flight arterial angiography; CBF: cerebral blood flow; *Other MRI acquisitions.

A metronome connected to the scanner's sound system was used to pace the respiration. The volunteers followed the described hyperventilation for pattern 5 min before the measurements were performed to ensure the hypoperfusion state was achieved and stable. Hyperperfusion was achieved by intravenous administration of ACZ (15-20 mg/kg, Diamox, Mercury Pharmaceuticals, London, UK) over a 5-min period. Post-ACZ scans were commenced 20 min after the end of ACZ administration.

Arterial blood samples were obtained at the end of each PET CBF measurement. Arterial blood gases, pH, and hemoglobin were analyzed in a Radiometer ABL800 Flex system (Radiometer, Copenhagen, Denmark). The arterial line was flushed with a heparin solution (100 i.u./mL. Leo Pharma, Ballerup, Denmark) after each scan to prevent clot formation. Respiratory rate was monitored with a respiration belt during the experiment, especially during the measurements in hyperventilation, to ensure that the volunteer was following the hyperventilation scheme. Pulse was monitored during the experiment using an MRI compatible finger pulse oximeter connected to the scanner for the pulse-triggered PCM MRI measurements. Arterial blood pressure was measured prior to the experiment, before and after the ACZ administration, and at the end of the experiment.

MRI

A 16-channel mMR head and neck coil designed by the vendor to minimize attenuation of the PET signal was used for all the MRI measurements.

Structural imaging

A high-resolution structural scan was obtained prior to the first CBF measurement using a 3D T1-weighted magnetization prepared rapid acquisition gradient echo (T1 MPRAGE) sequence (repetition time (time between pulses, TR) 1900 ms, echo time (TE) 2.44 ms, flip angle 9°, matrix 256×256, voxel size $1.0 \times 1.0 \times 1.0\,mm^3$, GRAPPA acceleration factor 2).

The anatomical scans were segmented using the FSL BET and FAST tools[20] in order to obtain a brain tissue mask including cerebral hemispheres, cerebellum and brain stem (and excluding the cerebrospinal fluid) used for the calculation of the total brain volume and to mask the PET CBF images. Brain weight was calculated assuming a brain tissue density of 1.05 g/mL.[21]

Flow measurements acquisition

A 3D time-of-flight (3D-TOF) angiogram (TR 22 ms, TE 3.60 ms, flip angle 18 degrees, matrix 256×232, FOV $200 \times 181\,mm^2$ and voxel size $0.8 \times 0.8 \times 1.0\,mm^3$) was performed prior to the PCM measurements in each state.

Pulse-triggered PCM measurements (single slice, TR 37.4 ms, TE 3.32 ms, flip angle 25°, FOV $320 \times 240\,mm^2$, voxel size $0.8 \times 0.8 \times 5.0\,mm^3$, 20 phases per cardiac cycle and averaging 2 measurements, velocity encoding (V_{enc}) of 150 cm/s performed only in the direction (superior-inferior) of the imaging plane) were commenced 7 min after the beginning of the PET scan (after other MRI perfusion measurements not included in the present analysis). The duration of the scan was approximately 2 min, and varied slightly from subject-to-subject depending on their heart rate. The 3D-TOF angiograms maximum intensity projections were used for the planning of PCM. A single PCM imaging plane was placed at the level of the upper part of the V2 segment of the vertebral arteries (VAs) and in the C1 segment of the internal carotid arteries (ICA), and angulated as perpendicular as possible to the four arteries, prioritizing optimal angulation of the ICAs (an example is provided in Supplementary material, Figure S1).

MRI post-processing

PCM generated three dynamic images: a magnitude image showing anatomy, a velocity image and a complex subtraction image. All PCM images were converted to NIfTI file format and processed using in-house software for MATLAB version R2016b (The Mathworks, Natick, MA, USA).

Average magnitude and velocity images were created by averaging the signal over all phases of the cardiac cycle. Regions of interest (ROIs) of the four brain feeding arteries were initially manually drawn on the average complex subtraction image and then transferred to the averaged velocity maps. To avoid the influence of vessel wall artefacts, voxels with an average negative velocity in the periphery of the vessel were excluded from the ROI. The ROIs were then copied to the dynamic velocity maps and visually inspected for aliasing and for voxels with erroneous flow velocity patterns. Flow was calculated by multiplying the mean velocity with the cross-sectional area of each ROI and then summation over 20 time-points was performed.

PET

Acquisition

For each PET scan, a bolus of approximately 500 MBq of ^{15}O-labelled water (^{15}O-H_2O) produced in an online system (Automatic Water Injection System, Scansys Laboratorieteknik, Værløse, Denmark) was manually injected in the median cubital vein. Emission scans were started at the time of the radiotracer injection and recorded in list mode for 4 min. At least 13 min passed between PET measurements to allow for the tracer decay.

PET images were reconstructed into 18×5 s, 9×10 s, 4×15 s frames using 3D-ordered subset expectation maximum (3D OSEM), 4 iterations 21 subsets, 128×128 matrix and 2 mm Gaussian filter. The attenuation correction was performed using μ-maps generated from the low-dose CT scan as previously described.[19]

Arterial blood sampling

Activity in the arterial blood was sampled at 1 Hz during the scans using an MR compatible automatic blood sampling system (Swisstrace, Zürich, Switzerland) set to draw 8 mL/min. Flow rate, material, length (50 cm) and diameter (1 mm) of the arterial line was identical to our current clinical and research setup on our brain dedicated PET scanner. The sampling system clock was synchronized to the scanner acquisition clock for the correct decay correction of the data. Blood sampling was started approximately 90 s prior to the radiotracer injection and was stopped 4 min after the beginning of the PET acquisition.

Post processing

Parametric images were generated with the software PMOD 3.304 (PMOD Technologies, Zürich, Switzerland) using a one tissue two-compartment model with correction for arterial blood volume fitting the first 180 s from bolus arrival to the brain of the dynamic sequence.[22,23] The arterial input curves were corrected for dead-time, decay, delay and dispersion. CBF is reported as the unidirectional clearance of tracer from the blood to the tissue (K_1) assuming full extraction of water. Each parametric CBF map was co-registered to its corresponding anatomical T1-MPRAGE, and the whole brain mask was applied to obtain gCBF calculated as the average of all voxels within the mask.

Statistics

Summary results for each state are presented including all the measurements. For reporting of summary statistics (Tables 1 to 3), the results of the duplicate measurements by each method were averaged in in each state. Results of PCM MRI flow measurements from both VAs and ICAs were also averaged. In all other analyses and plots, all individual measurements in each state were included.

For reporting of inter-state differences, only values from subjects that completed combined measurements in two states (post-ACZ and rest, and/or hyperventilation and rest) were included. Inter-state differences were defined as the difference between the individual non-resting state measurement (post-ACZ or in hyperventilation) and the average of the two resting state measurements. Differences between states or modalities were investigated using a Wilcoxon–Mann–Whitney test.

Method agreement was investigated by Bland–Altman plots and by linear mixed analysis. In order to take into account that multiple measurements were performed in each subject, associations of PCM MRI and ^{15}O-H_2O PET measurements of gCBF were investigated by a two-level linear mixed model with MRI PCM gCBF as dependent variable, ^{15}O-H_2O PET gCBF as fixed effect, and subject (μ, level 2) as random effects (and replicate measurement as residual, ϵ, level 1)

$$gCBF_{PCM} = \beta_0 + \beta_1 . gCBF_{PET} + \mu + \varepsilon$$

Identical models were analyzed for each state separately and for inter-state differences. Correlation coefficients (R^2 values) for all states combined, and for each state were calculated by comparing the sum of variance components in similar two-level variance component models with and without fixed effects.

In order to asses method precision, intra- and inter-individual variability (coefficient of variation, CV) of resting measurements was calculated as the standard deviations of the random effects (μ and ϵ, respectively, in a two-level linear mixed model similar to that above

Table 1. Cardiorespiratory variables during the experiment.

	Resting ($n = 26/14$)	Hyperventilation ($n = 17/9$)	Post-acetazolamide ($n = 19/10$)
Heart rate (min^{-1})	59.4 ± 8.3	66.8 ± 9.4^a	64.4 ± 10.9
Respiratory rate (min^{-1})	16.4 ± 2.0	24.2 ± 0.4^a	17.6 ± 1.8
pH	7.40 ± 0.01	7.54 ± 0.07^a	7.39 ± 0.03
P_aCO_2 (kPa)	5.8 ± 0.4	3.7 ± 0.8^a	5.5 ± 0.3^a
P_aO_2 (kPa)	13.8 ± 0.9	16.8 ± 1.6^a	14.0 ± 1.0
ctHB (mmol/L)	9.6 ± 0.7	9.4 ± 0.4	9.3 ± 0.4
SaO_2 (%)	97.8 ± 0.4	99 ± 0.4	97.7 ± 0.4

Note: Values are the average ± standard deviations of the two measurements in each condition. For each state, *n* indicates the number of observations/number of subjects.

[a] $p < 0.005$ for difference versus resting conditions.

$PaCO_2$: arterial pressure of CO_2; P_aO_2: arterial pressure of O_2; ctHB: concentration of hemoglobin; SaO_2: arterial saturation of O_2.

Table 2. Characteristics of phase-contrast mapping MRI measurements per vessel.

	Rest ($n = 26/14$)		Hyperventilation ($n = 17/9$)		Post-acetazolamide ($n = 19/10$)	
	ICA	VA	ICA	VA	ICA	VA
V_{max} (cm/s)	55.1 ± 9.3	30.6 ± 7.7	45.4 ± 9.1^a	27.4 ± 11.1^a	60.9 ± 11.9^a	33.8 ± 9.5^a
Flow (mL/min)	285.4 ± 58.3	92.0 ± 42.3	171.0 ± 46.2^a	48.0 ± 32.5^a	428.3 ± 121.3^a	139.4 ± 82.7^a
Contribution to gCBF (%)	38.0 ± 4.3	12.0 ± 4.9	39.5 ± 4.6	10.5 ± 5.5	37.9 ± 4.1	12.1 ± 5.5
Total flow (mL/min)	755 ± 146		435 ± 124^a		1124 ± 341^a	

Note: Values are the average ± standard deviation of the left and right arteries in each condition. For each state, *n* indicates the number of observations/number of subjects.

[a] $p < 0.005$ for differences versus resting conditions (within artery).

ICA: internal carotid arteries; VA: vertebral arteries; V_{max}: voxel peak velocity; gCBF: global cerebral blood flow.

Table 3. Averaged global cerebral blood flow assessed by ^{15}O-H_2O PET and phase-contrast mapping MRI.

	Resting ($n = 26/14$)	Hyperventilation ($n = 17/9$)	Post-acetazolamide ($n = 19/10$)
PCM MRI (mL/100 g/min)	58.5 ± 10.7^b (0.18)	$33.0 \pm 8.6^{a,b}$ (0.26)	$89.6 \pm 27.1^{a,b}$ (0.30)
Change vs. rest (mL/100 g/min)	–	-26.9 ± 9.5	31.3 ± 17.9
Change vs. rest (%)	–	-36.9 ± 19.6	52.4 ± 23.8
^{15}O-H_2O PET (mL/100 g/min)	38.6 ± 5.7^b (0.15)	$24.7 \pm 5.8^{a,b}$ (0.23)	$57.3 \pm 9.6^{a,b}$ (0.17)
Change vs. rest (mL/100 g/min)	–	-16.4 ± 10.5	19.4 ± 8.3
Change vs. rest (%)	–	-35.0 ± 10.2	52.5 ± 22.6

Note: All values are the average ± standard deviation of the two measurements in each condition, coefficient of variation in parenthesis. For each state, *n* indicates the number of observations /number of subjects. The change is calculated as the difference of the average gCBF in resting state and in hyperventilation or after acetazolamide. Only subjects with measurements in at least two states contribute the calculation of gCBF changes.

[a] $p < 0.05$ for differences with resting state, within technique.

[b] $p < 0.05$ for differences between techniques, within state.

PCM MRI: phase contrast mapping magnetic resonance imaging; PET: positron emission tomography; gCBF: global cerebral blood flow.

with either $gCBF_{PET}$ or $gCBF_{PCM}$ as outcome and including only measurement number as fixed effect) divided by the population mean.

Results

Nine of the fourteen volunteers had measurements performed in all three states. In one volunteer, measurements during hyperventilation were omitted due to the time restrictions. In the remaining volunteers that did not complete the scanning protocol, this was prematurely terminated due to the clotting of the arterial line ($n = 3$), or at the request of the volunteer ($n = 1$). In total, 62 paired observations were performed by PET/MRI: 26 measurements in resting state in 14 volunteers, 17 measurements during hyperventilation in 9 volunteers, and 19 measurements after administration of ACZ in 10 volunteers. Two combined measurements were discarded due to the suboptimal data quality of PCM MRI measurements as a consequence of excessive head movement at the end of the experiment.

Physiological measurements in the three different states are shown in Table 1. During hyperventilation, there was a reduction of 0.6 kPa in the average P_aCO_2 in the second measurement compared to the first one ($p < 0.005$). Hyperventilation significantly decreased P_aCO_2 and increased heart rate, pH and P_aO_2. After the administration of ACZ, a small, but significant decrease in P_aO_2 was observed along with a slight, but non-significant, increase in the respiratory rate.

The average brain tissue volume was 1347 ± 77 mL. The results of the PCM MRI measurements for each vessel in the three different states are shown in Table 2. No aliasing was observed in any of the PCM MRI measurements. The range of fitted delay and dispersion values of the ^{15}O-H_2O input function was 9–15 s and 5–6 s, respectively, corresponding to what we obtain using the same arterial line and kinetic models in healthy men scanned in a dedicated brain PET HRRT scanner. Examples of CBF measured by ^{15}O-H_2O PET and PCM MRI in each state are shown in Figure 2

Values of gCBF assessed by PCM MRI and ^{15}O-H_2O PET in the three different states are summarized in Table 3. Overall, a highly significant positive correlation of PCM MRI with ^{15}O-H_2O PET across all states was observed. Within each state, the correlation between methods was generally weaker, but statistically significant for rest and post-ACZ states (Figure 3(a) and Table 4).

PCM MRI yielded higher gCBF values compared to ^{15}O-H_2O PET: 47.7% on average across all states, and 35.9%, 51.5% and 53.7% on average during hyperventilation, in rest and after ACZ, respectively. Figure 3(a) demonstrates a relative, perfusion-dependent increase in the difference between the PCM MRI and the ^{15}O-H_2O PET gCBF values. This is confirmed by the Bland–Altman plot (Figure 3(b)) also showing that the *relative* difference increases with increasing perfusion. The positive slope corresponds to a 0.7%-point increase in the relative difference between PCM MRI and ^{15}O-H_2O PET per mL/100 g/min increase in the average of the two techniques, i.e. 26% at an average of 20 mL/100 g/min and 69% at 80 mL/100 g/min. The estimate of the regression coefficient in each state tended to be lower than the overall estimate (Table 4). Scatter plots of gCBF measured by PCM MRI and by ^{15}O-H_2O PET for each individual state can be found in the Supplementary Material (Figure S2).

The agreement of PCM MRI with ^{15}O-H_2O PET for the quantification of absolute gCBF *changes* from baseline to hyperventilation and after ACZ was in general poorer, with weak correlation and borderline significance (Table 4 and Figure S3).

Intrasubject variability (CV) of gCBF in resting state was 6.2% for PCM MRI and 6.4% for ^{15}O-H_2O PET. The corresponding CVs of intersubject variability were 17.0% and 13.6%, respectively.

Discussion

The present study is unique by obtaining multiple combined PCM MRI and fully quantitative ^{15}O-H_2O PET gCBF measurements with arterial blood sampling in healthy volunteers across different perfusion states in a single imaging session using a hybrid PET/MRI system. The most important contribution of single scan session PET and MRI (near-) simultaneous imaging is achieving the best possible matching of physiological parameters known to influence CBF, e.g. arterial blood gasses, pH, hemoglobin, caffeine levels, and sensitivity to ACZ,[17,24] that will be challenging to match in a dual scan session set-up.[25] The study shows a strong correlation between the PCM MRI and ^{15}O-H_2O PET gCBF over a wide range of perfusion values confirming the capability of PCM MRI to provide quantitative gCBF measurements, also at lowered and increased perfusion. However, we also found a perfusion-dependent increasing relative difference with PCM MRI yielding higher gCBF values compared to ^{15}O-H_2O PET, and relatively poor agreement with regard to quantitation of gCBF changes. The study demonstrates the potential of hybrid PET/MRI scanners to perform intra-session physiological measurements independently, and importantly also that it is possible to perform such measurements involving a complex setup despite the physical limitations of the experimental environment.

The average gCBF in resting state measured by PCM MRI (58.5 ± 10.1 mL/100 g/min) and by ^{15}O-H_2O PET (38.6 ± 5.71 mL/100 g/min) is over- and

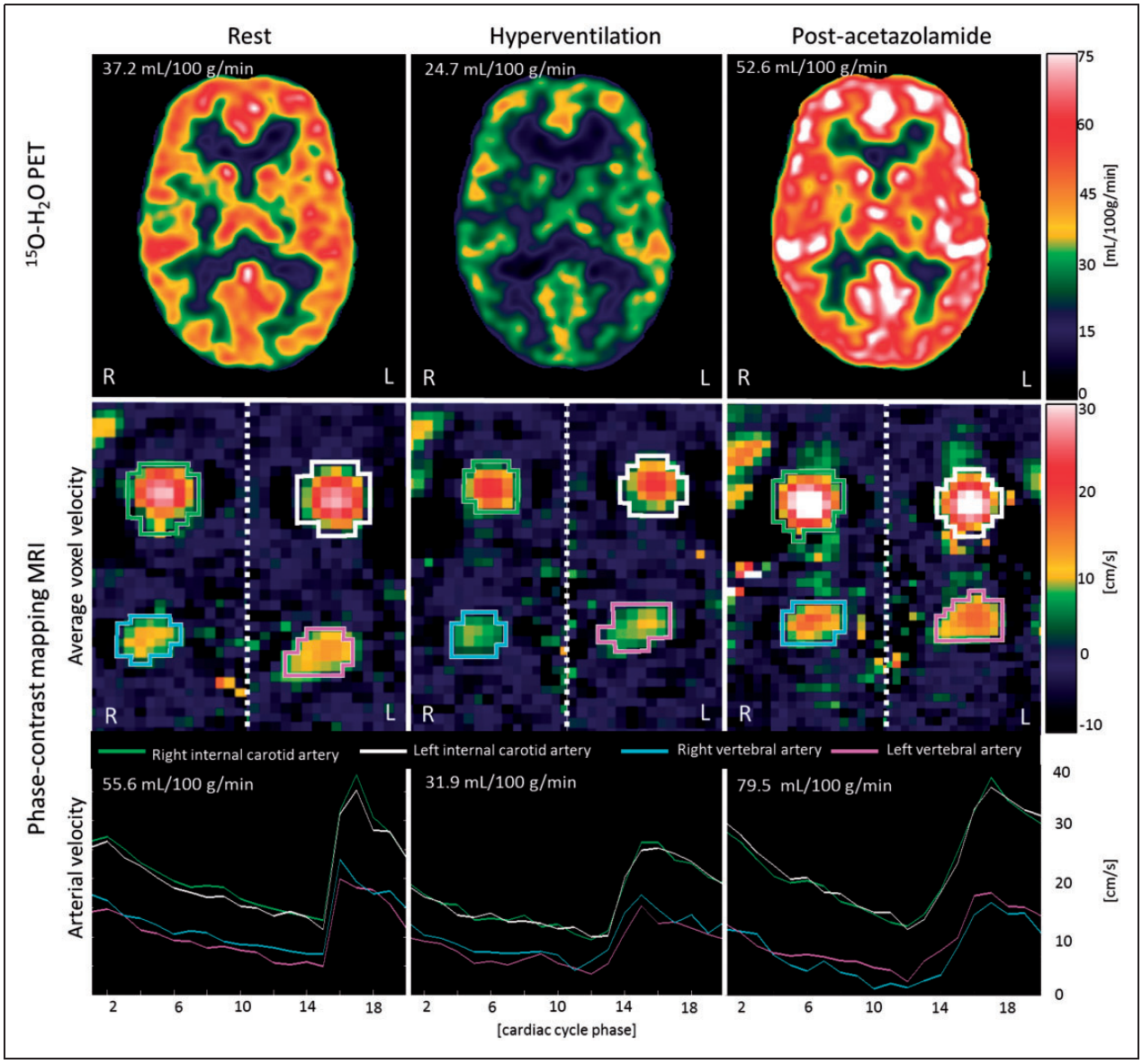

Figure 2. Examples CBF measurements. Panels show ^{15}O-H$_2$O PET CBF images (top row), PCM MRI average velocity images across the cardiac cycle (middle row) and arterial mean velocity of each vessel over the cardiac cycle (bottom row) in each state from a single volunteer. Colored ROI for each vessel are displayed over the average velocity images and the corresponding arterial flow over the cardiac cycle is shown below. L: left; R: right.

underestimated, respectively, compared to the generally accepted text book value for resting gCBF around 46–50 mL/100 g/min.[26,27] They are, however, in good agreement with those reported previously by other authors using identical methods,[13,28] confirming the correct implementation of the measurement techniques. The absolute gCBF increase after the administration of ACZ measured by PCM MRI and by ^{15}O-H$_2$O PET is also in good agreement with published studies.[28,29]

The study confirms the previous finding of a large and systematic relative difference in the order of 50% between PCM MRI and ^{15}O-H$_2$O PET reported by Vestergaard et al.[15] In our study, the correlation between methods in resting state was lower than that reported by Vestergaard et al. ($R^2 = 0.17$ vs. 0.44).[15] The lower correlation coefficient could to some extent reflect random variation due to the lower number of independent measurements in the present study. The intrasubject variability of approximately 6% for both techniques, however, is very similar to that reported by Vestergaard et al (6.5% for PCM MRI and 5.7% for ^{15}O-H$_2$O PET) and does not suggest increased method imprecision as a cause of the observed lower correlation. The slope of the linear fit in the study of

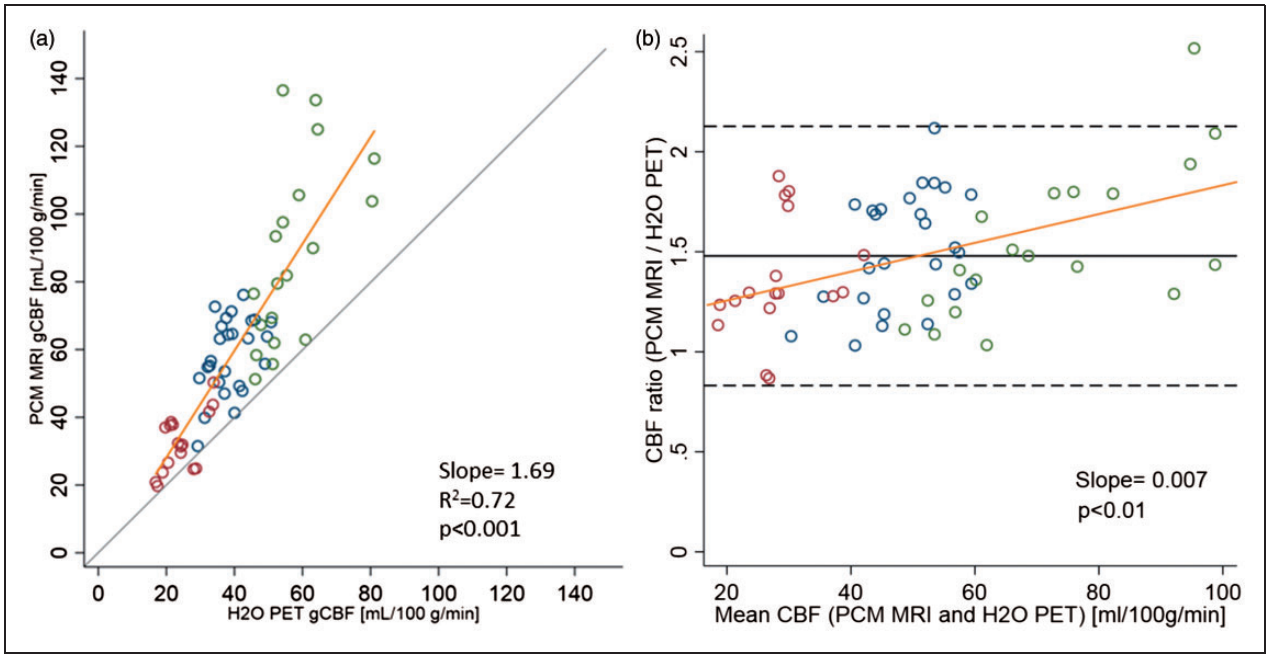

Figure 3. Correlation of gCBF measurements by ^{15}O-H_2O PET and PCM MRI. (a) Scatter plot of global cerebral blood flow (gCBF) measured by ^{15}O-H_2O PET and phase-contrast mapping (PCM) MRI during hyperventilation (red), in rest (blue) and after acetazolamide (green). (b) Bland–Altman plot showing the *ratio* of the two methods against mean of the methods. Yellow line shows the linear fit from the mixed model. In 3(a), grey line indicates the line of identity. In 3(b), solid grey and dashed lines indicate bias upper and lower limits of agreement (bias ± 2 SD), respectively.

Table 4. Association of global cerebral blood flow measurements by ^{15}O-H_2O PET and PCM MRI.

	Estimate (95% CI)	*p*	R^2
All states	1.69 (1.55; 1.82)	<0.001	0.72
Rest	0.89 (0.28; 1.50)	0.008	0.17
Hyperventilation	0.87 (−0.06; 1.81)	0.063	0.33
Change from rest	0.46 (−0.03; 0.95)	0.061	0.08
Rel. change from rest	0.47 (0.26; 0.68)	<0.001	0.33
Post-acetazolamide	1.30 (0.38; 2.22)	0.011	0.33
Change from rest	1.02 (−0.07; 2.12)	0.064	0.07
Rel. change from rest	0.61 (−0.18; 1.42)	0.11	<0.001

Note: Estimate represents regression coefficient in the two-level mixed model. Changes are calculated as absolute and relative change from average of the two resting measurements to each subsequent measurement. CI: confidence interval; PCM MRI: phase contrast mapping magnetic resonance imaging; PET: positron emission tomography.

Vestergaard et al. is somewhat steeper, but well within the confidence interval of the estimate of the rest measurements in the present study (1.32 vs. 0.89 [CI: 0.28–1.50]). We therefore conclude that the findings of the present study are not in conflict with the previous study from Vestergaard et al.

The basis of the PCM MRI and ^{15}O-H_2O PET gCBF difference has been discussed in details previously[15] and can, in large, be attributed to systematic overestimation of flow measured by PCM MRI and underestimation by ^{15}O-H_2O PET.

For PCM MRI, partial volume effects may lead to an overestimation of the measured flow in particular if the vessel diameter is low compared to image resolution or when measurements are not performed perpendicular to the vessel.[30,31] We used a single imaging plane to measure the arterial flow in all four arteries, which might lead to a sub-optimal positioning of the plane for the measurements of some of the vessels. For this reason, we prioritized correct positioning of the imaging plane of the ICAs contributing to almost 80% of the total cerebral flow. We also found that the flow distribution between ICAs and VAs is constant across perfusion states which support linearity between the measured flow and true flow.

Underestimation of the ^{15}O-H_2O PET gCBF measurements may largely be explained by the limited water extraction fraction across the blood–brain barrier (approximately 0.85 at resting CBF values) when quantifying CBF from ^{15}O-H_2O PET using the unidirectional clearance rate constant, K_1, of a one-tissue two-compartment model.[32] The diffusion limitation has the most pronounced effect at high CBF values, which probably explains the observed perfusion-dependent difference values of PCM MRI compared to ^{15}O-H_2O PET.

For this study, a fixed V_{enc} of 150 cm/s was used in all measurements in order to maintain the scanning protocol throughout the different measurements and to prevent aliasing in high flow measurements. Our results show a mean peak voxel velocity of 60.9 ± 11.9 cm/s in the ICAs after the administration of ACZ, and the highest voxel peak velocity measured was 87 cm/s. The use of a V_{enc} of 150 cm/s seems to be excessive for this experiment,[33] a V_{enc} of approximately 100 cm/s would be reasonable when scanning healthy young volunteers in different perfusion states.

It is noteworthy that the slope (the regression coefficient estimate) in rest differs from the overall slope and the confidence intervals do not overlap. However, it should also be noted that the estimates in each of the three states are overlapping and tend to be lower than the overall estimate and not significantly different from one. In a post hoc analysis, applying three-level random effects model with interaction term failed to demonstrate significant state-dependent differences. We interpret this as the overall slope mainly reflects the general approx. 50% difference between methods and that a common intercept is forced upon data when applying a single linear fit. Analyzing each state separately allows a better fit of data with state specific intercepts and a slope closer to optimal value of one in each state. The slightly lower than one slope in rest and hyperventilation could be the consequence of statistical attenuation bias due to method imprecision of the PET measurements, whereas the steeper slope in post-ACZ measurements can be attributed to the limited water extraction at higher perfusion values.

The present study has some limitations. First of all, MRI and PET data were acquired in close sequence, but not completely simultaneously. However, the time span was less than 10 min and there were no significant differences between the repeated gCBF PET measurements within each state, indicating physiologic stability. Another limitation is the limited number of subjects studied and the relatively high number of incomplete studies as a consequence of the complexity of the setup. Although the study population was relatively small, it is compensated by multiple paired measurements in different perfusion states using repeated tracer injection. This means that the number of paired measurements exceeds the number obtained in the largest previously published study comparing of CBF measurement using PCM MRI and ^{15}O-H_2O PET (performed in two separate sessions) by a factor of 3.[15] It was therefore concluded that the overall findings were robust and would not have changed by increasing number of subjects.

The relatively high proportion of incomplete studies due to arterial line clotting in 3/14 sessions was possibly related to the suboptimal wrist position due to the physical constrains at the edge of the bore opening. This supports the perception that quantitative ^{15}O-H_2O PET is a technically challenging procedure to perform. For these reasons, it would be convenient to have an alternative technique to simplify or substitute it. In the same way as PCM MRI measurements may be used to scale relative perfusion maps by ASL,[11] PCM MRI could also be used to scale relative ^{15}O-H_2O PET perfusion maps, thereby replacing arterial blood sampling. Doing so would potentially overcome the errors related to limited water extraction and this approach has been studied in piglets.[17] It should be noted though, that the actual flow values obtained by PCM MRI are highly dependent on in-plane resolution[30,31] and may even vary between sites although using identical MR systems and acquisition parameters[13] meaning that there is still no generally accepted standard acquisition protocol for PCM MRI.

The poorer correlation of absolute gCBF changes at the single subject level compared to the study population level is most likely due to method-imprecision and bias from both the methods in both states. Analyzing relative changes, the correlation of hyperventilation-induced hypoperfusion was greatly improved, but the correlation of gCBF changes after ACZ, however, remained poor. This is most likely related to the decreasing water extraction fraction in the hyperperfusion state. The weak correlation between the techniques for quantification of between-states gCBF changes suggests that PCM MRI and ^{15}O-H_2O PET measurement of gCBF changes cannot be used interchangeably at the single subject level due to their different behavior at high perfusion states. It has to be noted, however, that despite its limitations, gCBF changes assessed by ^{15}O-H_2O PET have been extensively validated clinically and in physiological experiments.[28,34] Further investigations are required if PCM-scaled relative CBF maps are to be applied for clinical assessment of regional flow reserve.

Additionally, any systematic perfusion-dependent biases in gCBF PCM MRI measurements will propagate into any calculation of derived physiological measurements such as $CMRO_2$.[6] The particular relationship between ^{15}O-H_2O PET and PCM gCBF measurements needs to be acknowledged when replacing ^{15}O-H_2O PET with PCM MRI in quantitative studies of brain physiology. The observed non-linear bias can largely be explained by the method-related bias as discussed above, and PCM MRI may provide a more linear correlation with true CBF at high flow values than ^{15}O-H_2O, although the latter cannot be determined from the presents study.

In conclusion, this study shows that PCM MRI and ^{15}O-H_2O PET gCBF measurements performed in close sequence across different perfusion states are highly correlated, which confirms the ability of PCM MRI

to perform gCBF measurements. The data, however, also confirmed considerable and perfusion-dependent relative bias between the two techniques. Finally, this study demonstrates the potential of hybrid PET/MRI systems to perform multiple paired intra-session quantitative physiological measurements independently, which is crucial for MRI validation studies when using PET as reference.

Funding

The author(s) disclosed receipt of the following financial support for the research, authorship, and/or publication of this article: OP is supported by a training grant from the Fundación Alfonso Martín Escudero and MBV is supported by a post-doc grant from the Danish Council for Independent Research (reference number: 6110-00692A).

Acknowledgments

The authors would like to thank the hard work and dedication of the nuclear medicine technologists and radiographers Nadia Azizi, Marianne Federspiel, Jakup Poulsen and Karin Stahr; the staff of the Cyclotron and Radiochemistry Unit, and the Trauma Center for the assistance with the arterial blood gases analysis. We also thank Julie Lyng Forman from the Department of Biostatistics, University of Copenhagen for her assistance. We would also like to thank The John and Birthe Meyer Foundation, who generously donated the PET/MRI scanner and the cyclotron to Copenhagen University Hospital Rigshospitalet.

Declaration of conflicting interests

The author(s) declared no potential conflicts of interest with respect to the research, authorship, and/or publication of this article.

Authors' contributions

OP contributed to the design of the study, acquisition, analysis and interpretation of the data, and the drafting of the article. MVB, UL and AEH contributed in the acquisition, analysis and interpretation of the data, and the drafting. AU and HHJ contributed in the acquisition of the data. FLA contributed in the design of the study and the analysis of the data. ER contributed to the design of the study, analysis and interpretation of the data, and the drafting of the article. HBWL contributed to de design, interpretation of the data and drafting of the article. IL and OMH contributed to the design of the study, acquisition, analysis and interpretation of the data, and the drafting of the article. All authors revised critically the draft and approved the version to be published.

Supplementary material

Supplementary material for this paper is available at: http://jcbfm.sagepub.com/content/by/supplemental-data.

ORCID iD

Oriol Puig http://orcid.org/0000-0002-3510-9204

References

1. Wintermark M, Sesay M, Barbier E, et al. Comparative overview of brain perfusion imaging techniques. *Stroke* 2005; 36: e86–99.
2. Spilt A, Box FM, Van Der Geest RJ, et al. Reproducibility of total cerebral blood flow measurements using phase contrast magnetic resonance imaging. *J Magn Reson Imaging* 2002; 16: 1–5.
3. Vernooij MW, Van Der Lugt A, Ikram MA, et al. Total cerebral blood flow and total brain perfusion in the general population: the Rotterdam Scan Study. *J Cereb Blood Flow Metab* 2008; 28: 412–419.
4. Appelman AP, Van Der Graaf Y, Vincken KL, et al. Total cerebral blood flow, white matter lesions and brain atrophy: the SMART-MR study. *J Cereb Blood Flow Metab* 2008; 28: 633–639.
5. Coverdale NS, Gati JS, Opalevych O, et al. Cerebral blood flow velocity underestimates cerebral blood flow during modest hypercapnia and hypocapnia. *J Appl Physiol* 2014; 117: 1090–1096.
6. Xu F, Ge Y and Lu H. Non-invasive quantification of whole-brain cerebral metabolic rate of oxygen by MRI. *Magn Reson Med* 2010; 39: 115–123.
7. Peng S-L, Dumas JA, Park DC, et al. Age-related increase of resting metabolic rate in the human brain. *Neuroimage* 2014; 98: 176–183.
8. Liu P, Huang H, Rollins N, et al. Quantitative assessment of global cerebral metabolic rate of oxygen (CMRO2) in neonates using MRI. *NMR Biomed* 2014; 27: 332–340.
9. Vestergaard MB and Larsson HB. Cerebral metabolism and vascular reactivity during breath-hold and hypoxic challenge in freedivers and healthy controls. *J Cereb Blood Flow Metab*. Epub ahead of print 3 November 2017. DOI: 0271678X1773790.
10. Bonekamp D, Degaonkar M and Barker PB. Quantitative cerebral blood flow in dynamic susceptibility contrast MRI using total cerebral flow from phase contrast magnetic resonance angiography. *Magn Reson Med* 2011; 66: 57–66.
11. Zhang K, Herzog H, Mauler J, et al. Comparison of cerebral blood flow acquired by simultaneous [15O]water positron emission tomography and arterial spin labeling magnetic resonance imaging. *J Cereb Blood Flow Metab* 2014; 34: 1373–1380.
12. Aslan S, Xu F, Wang PL, et al. Estimation of labeling efficiency in pseudocontinuous arterial spin labeling. *Magn Reson Med* 2010; 63: 765–771.
13. Dolui S, Wang Z, Wang DJ, et al. Comparison of non-invasive MRI measurements of cerebral blood flow in a large multisite cohort. *J Cereb Blood Flow Metab* 2016; 36: 1244–1256.
14. Henriksen OM, Larsson HBW, Hansen AE, et al. Estimation of intersubject variability of cerebral blood flow measurements using MRI and positron emission tomography. *J Magn Reson Imaging* 2012; 35: 1290–1299.
15. Vestergaard MB, Lindberg U, Aachmann-Andersen NJ, et al. Comparison of global cerebral blood flow measured by phase-contrast mapping MRI with ^{15}O-H_2O positron

emission tomography. *J Magn Reson Imaging* 2017; 45: 692–699.
16. Fan AP, Jahanian H, Holdsworth SJ, et al. Comparison of cerebral blood flow measurement with [15O]-water positron emission tomography and arterial spin labeling magnetic resonance imaging: a systematic review. *J Cereb blood flow Metab* 2016; 36: 842–861.
17. Andersen JB, Henning WS, Lindberg U, et al. Positron emission tomography / magnetic resonance hybrid scanner imaging of cerebral blood fl ow using 15 O-water positron emission tomography and arterial spin labeling magnetic resonance imaging in newborn piglets. *J Cereb Blood Flow Metab* 2015; 35: 1703–1710.
18. Addicott MA, Yang LL, Peiffer AM, et al. The effect of daily caffeine use on cerebral blood flow: how much caffeine can we tolerate? *Hum Brain Mapp* 2009; 30: 3102–3114.
19. Andersen FL, Ladefoged CN, Beyer T, et al. Combined PET/MR imaging in neurology: MR-based attenuation correction implies a strong spatial bias when ignoring bone. *Neuroimage* 2014; 84: 206–216.
20. Zhang Y, Brady M and Smith S. Segmentation of brain MR images through a hidden Markov random field model and the expectation-maximization algorithm. *IEEE Trans Med Imag* 2001; 20: 45–57.
21. Torack R, Alcala H, Gado M, et al. Correlative assay of computerized cranial tomography (CCT), water content and specific gravity in normal and pathological postmortem brain. *Neuropathol Exp Neurol* 1976; 35: 385–392.
22. Ohta S, Meyer E, Fujita H, et al. Cerebral [15O] water clearance in humans determined by PET: I. Theory and normal values. *J Cereb Blood Flow Metab* 1996; 16: 765–780.
23. Fujita H, Meyer E, Reutens D, et al. Cerebral [15O] water clearance in humans determined by positron emission tomography: II. Vascular responses to vibrotac-tile stimulation. *J Cereb Blood Flow Metab* 1997; 17: 73–79.
24. Andersen JB, Lindberg U, Olesen OV, et al. Hybrid PET/MRI imaging in healthy unsedated newborn infants with quantitative rCBF measurements using ^{15}O-water PET. *J Cereb Blood Flow Metab*, Epub ahead of print 15 January 2018. DOI: 10.1177/0271678X17751835.
25. Heijtel DFR, Mutsaerts HJMM, Bakker E, et al. Accuracy and precision of pseudo-continuous arterial spin labeling perfusion during baseline and hypercapnia: a head-to-head comparison with 15O H2O positron emission tomography. *Neuroimage* 2014; 92: 182–192.
26. Lassen NA. Normal average value of cerebral blood flow in younger adults is 50 ml/100 g/min. *J Cereb blood flow Metab* 1985; 5: 347–349.
27. Madsen PL, Holm S, Herning M, et al. Average blood-flow and oxygen-uptake in the human brain during resting wakefulness – a critical-appraisal of the Kety-Schmidt technique. *J Cereb Blood Flow Metab* 1993; 13: 646–655.
28. Okazawa H, Yamauchi H, Sugimoto K, et al. Effects of acetazolamide on cerebral blood flow, blood volume, and oxygen metabolism: a positron emission tomography study with healthy volunteers. *J Cereb Blood Flow Metab* 2001; 21: 1472–1479.
29. Spilt A, Van Den Boom R, Kamper AM, et al. MR assessment of cerebral vascular response: a comparison of two methods. *J Magn Reson Imaging* 2002; 16: 610–616.
30. Tang C, Blatter D and Parker D. Accuracy of phase-contrast flow meas- urements in the presence of partial-volume effects. *J Magn Reson Imaging* 1993; 3: 377–385.
31. Peng SL, Su P, Wang FN, et al. Optimization of phase-contrast MRI for the quantification of whole-brain cerebral blood flow. *J Magn Reson Imaging* 2015; 42: 1126–1133.
32. Paulson O, Hertz M, Bolwig T, et al. Filtration and diffusion of water across the blood-brain barrier in man. *Microvasc Res* 1977; 1: 113–124.
33. Lotz J, Meier C, Leppert A, et al. Cardiovascular flow measurement with phase-contrast mr imaging: basic facts and implementation. *Radiographics* 2002; 22: 651–671.
34. Okazawa H, Yamauchi H, Toyoda H, et al. Relationship between vasodilatation and cerebral blood flow increase in impaired hemodynamics: a PET study with the acetazolamide test in cerebrovascular disease. *J Nucl Med* 2003; 1875–83.